Infrared Physics & Technology 55 (2012) 363–367

Contents lists available at SciVerse ScienceDirect

Infrared Physics & Technology

journal homepage: www.elsevier.com/locate/infrared

Reconstruction of size and depth of simulated defects in austenitic steel plate using pulsed infrared thermography

Olga Wysocka-Fotek [a,*], Wiera Oliferuk [a,b], Michał Maj [a]

[a] Institute of Fundamental Technological Research, Polish Academy of Sciences, Pawińskiego 5B, 02-106 Warsaw, Poland
[b] Bialystok University of Technology, Wiejska 45, 15-351 Białystok, Poland

ARTICLE INFO

Article history:
Received 14 September 2011
Available online 27 February 2012

Keywords:
Pulsed IR thermography
Temperature time derivative
Defect size
Thermal contrast
Defect depth

ABSTRACT

In this paper the size and depth (distance from the tested surface) of defects in austenitic steel were estimated using pulse infrared thermography. The thermal contrast calculated from the surface distribution of the temperature is dependent on both these parameters. Thus, two independent experimental methods of defect size and depth determination were proposed. The defect size was estimated on the basis of surface distribution of the time derivative of the temperature, whereas the defect depth was assessed from the dependence of surface thermal contrast vs. cooling time.

1. Introduction

The application of active infrared (IR) thermography for detection of subsurface defects of the tested material needs a thermal stimulation of its surface. One of the active thermography techniques is a pulsed IR thermography where the surface of tested specimen is stimulated by a heat pulse and its self-cooling process is analyzed [1–8]. During this process the temperature decrease rate is different for surface over defect in comparison with that over the sound material. It is caused by a difference in values of thermal effusivity between defected zone and the sound one.

The unique features of the pulsed IR thermography are non-contact operation and high inspection speed. The method can be applied for detection of subsurface defects having different thermal properties with respect to the sound material (delaminations, cracks, voids, etc.).

The thermal effusivity of given material is defined as:

$$e = \sqrt{k\rho c}, \tag{1}$$

where k is thermal conductivity, ρ is mass density and c is specific heat of the material. The heat flow through the interface between two media is controlled by the ratio of their effusivities. In case of defected material, if the effusivity of defect is lower than the effusivity of matrix, the surface temperature over defect will be higher comparing to that over the sound material. Thus, by measuring the surface distribution of temperature of tested material, the defect presence can be revealed.

As the quantitative measure of the difference between values of the surface temperature over defected zone and over the sound material the standard thermal contrast $C(t)$ is used [9]:

$$C(t) = \frac{T_{def}(t) - T_{def}(t_0)}{T_s(t) - T_s(t_0)}, \tag{2}$$

where T_{def} is the surface temperature over defect, T_s is the surface temperature over the sound material, t_0 is the time just before pulse heating and t is the current time of the cooling process.

It has been shown that the relation of thermal contrast vs. cooling time has a maximum [1,3,7,8]. It can be explained in the following way: After pulse heating of the material containing the defect with lower thermal effusivity compared to the effusivity of matrix, the thermal contrast on the surface rises and then reaches the maximum, what is caused by increase of the internal energy of the area over defect. The decrease of thermal contrast is connected with achieving thermodynamic equilibrium between the different areas of the tested material.

The time related to the thermal contrast maximum is dependent on both size of defect and its depth [10,11]. Thus, the time corresponding to the standard thermal contrast maximum can be the same for defects with different depth and size, as it is seen in Fig. 1 [11]. It means that in order to determine the defect depth on the basis of the time of thermal contrast maximum it is necessary to know the defect size or to find a parameter dependent only on the defect depth. In the literature, the time corresponding to the maximum slope of thermal contrast (peak slope time) is proposed as the parameter independent on the defect size [7,12,13].

* Corresponding author. Tel.: +48 22 8261281x177; fax: +48 022 8269815.
E-mail addresses: owysocka@ippt.gov.pl (O. Wysocka-Fotek), wolif@ippt.gov.pl (W. Oliferuk), mimaj@ippt.gov.pl (M. Maj).

1350-4495/$ - see front matter © 2012 Elsevier B.V. All rights reserved.
doi:10.1016/j.infrared.2012.02.004

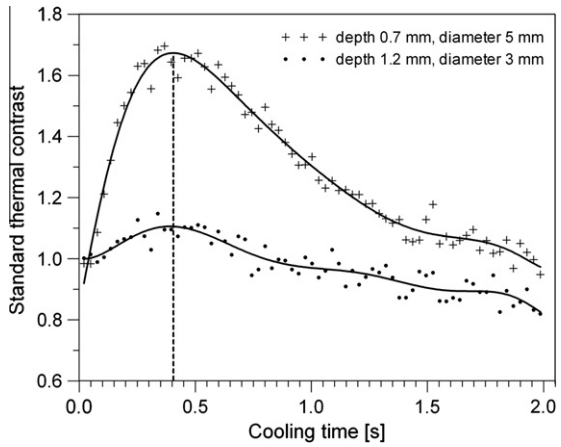

Fig. 1. The time of the standard thermal contrast maximum can be the same for defects with different depths and sizes. The experiment was performed on the austenitic steel plate with flat-bottom holes.

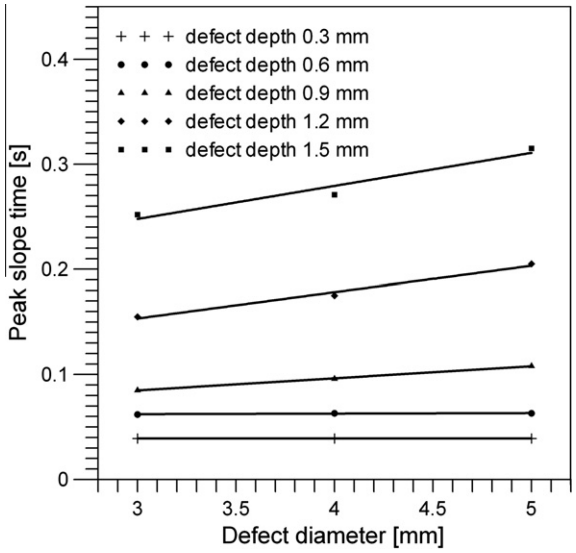

Fig. 2. Peak slope time of thermal contrast vs. defect diameter dependence. The experiment was performed on the austenitic steel with flat-bottom holes.

However, the results of experiments performed in the present work shows that it is true only for the defects with a high ratio of defect size to its depth (Fig. 2). Thus, to asses the defect depth on the basis of the time corresponding to the thermal contrast maximum, it is necessary to find an independent method of defect size determination. The objective of this work is to propose such method and to reconstruct the size and depth of simulated defects in austenitic steel plate.

2. Experimental procedure

The specimen made of 316L austenitic steel plate (250 mm × 300 mm × 5 mm) with flat-bottom holes was prepared. The diameters of defects were equal to: 3, 4, 5, 10 mm and were located at the different depths (Fig. 3). The specimen was coated by graphite paint in order to ensure high and homogeneous surface emissivity. The surface of the specimen was uniformly heated using the halogen lamp of the pulse energy of 6 kJ. Pulse duration was 3 ms and the lamp to specimen distance was equal to 0.5 m. The surface temperature distribution vs. cooling time was measured by ThermaCam Phoenix infrared thermographic system with InSb detector. The spectral range of the detector was 3–5 μm. The thermal sensitivity of the system at 25 °C is 20 mK. The thermal images (320 × 256 pixels) were recorded with the frequency 346 Hz. Both the IR camera and stimulating lamp were located at the same side of the specimen (Fig. 4).

3. Results and discussion

On the basis of time dependence of temperature distribution on the tested surface, the thermal contrasts (Eq. (2)) vs. cooling time for defects of different size and depth were calculated. Such dependences for the defect size of 3 mm located at the different depths are shown in Fig. 5. It is seen that the smaller depth of the defect corresponds to higher value of thermal contrast maximum and the shorter time to reach the maximum. It should be noticed that the obtained results are reliable only when the temperature distribution on the tested surface is not influenced by the opposite surface of the specimen. The range of cooling time, in which there is no such influence, was determined. It was done using the solution of the differential heat conduction equation for the homogenous semi-infinite body whose surface was heated uniformly by a pulse with infinitesimal duration. Assuming that after heat stimulation the cooling process of the surface is caused only by heat conduction, the solution for the surface of considered body has the form [14]:

$$\Delta T(t) = T(t) - T_0 = \frac{Q}{c\rho\sqrt{\pi}\sqrt{\alpha}} \cdot \frac{1}{\sqrt{t}}, \tag{3}$$

where $T(t)$ and T_0 are the temperature values of the tested surface after and before heat stimulation, Q is the surface density of the absorbed energy, t is the cooling time and α is the thermal diffusivity of the material.

On logarithmic scale the graph of function (3) for the sound material is a straight line with the slope equals to $-\frac{1}{2}$:

$$\ln[\Delta T(t)] = \ln\left(\frac{Q}{c\rho\sqrt{\pi}\sqrt{\alpha}}\right) - \frac{1}{2}\ln(t). \tag{4}$$

The dependence of $\ln[\Delta T(t)]$ on $\ln(t)$ for the plate of sound material (316L steel) with the thickness of 5 mm is presented in Fig. 6.

It is seen that up to $\ln(t) = 0.6$, what corresponds to cooling time $t = 1.8$ s, the graph is the straight line with slope equals to $-\frac{1}{2}$. It means, that in the time period from 0 to 1.8 s the tested plate can be treated as semi-infinite body. In other words, in this period the thermal contrast on the tested surface is not influenced by the opposite surface. It is noteworthy, that in general case, this time period depends not only on the specimen thickness but also on the thermal diffusivity of tested material. In the presented work, only these simulated defects were considered for which the times of the thermal contrast maximum were shorter then 1.8 s.

From the dependences of the standard thermal contrast on the cooling time for different diameters of simulated defects, the calibration relations have been created. These are relations between defect depth and the time corresponding to the thermal contrast maximum. Such relations for all simulated defects are presented in Fig. 7. It is seen that for every defect diameter this dependence is a straight line with the same slope. Obtained results are not consistent with that presented in the paper [12], where authors maintain that the time of thermal contrast maximum is a linear function of the squared depth. Nevertheless, the most of experimental results are in accordance with that presented in Fig. 7 [10,15,16].

To determine the defect depth on the basis of obtained calibration relations it is necessary to know the size of the defect. Therefore, an independent method of the defect size estimation is proposed.

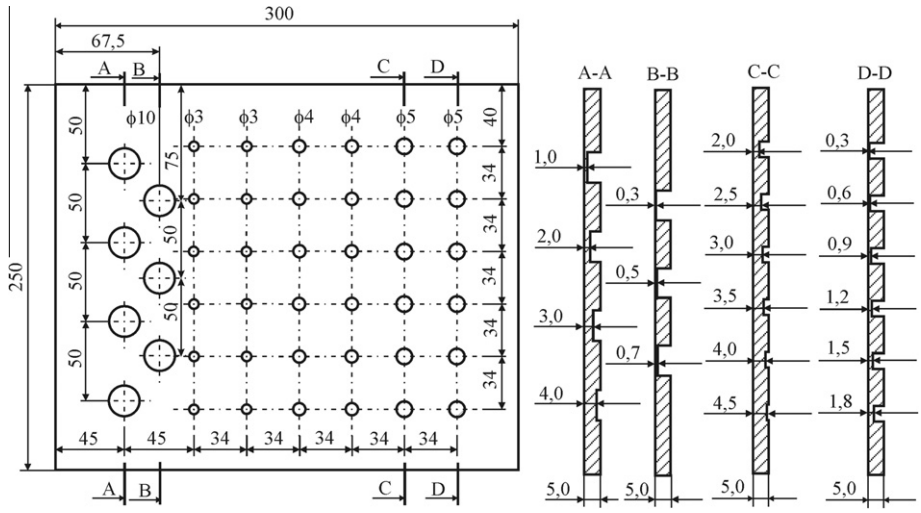

Fig. 3. The geometry of the steel plate with simulated defects.

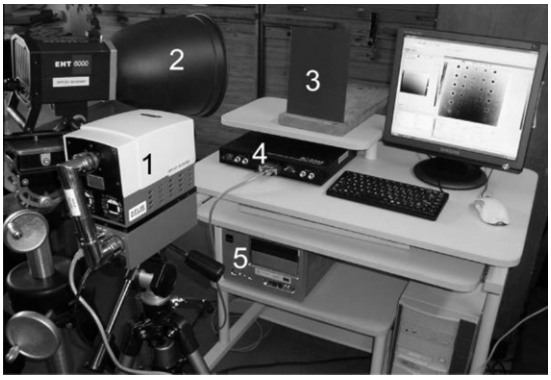

Fig. 4. Experimental set-up for pulsed thermography: 1 – IR camera, 2 – flash lamp, 3 – tested specimen, 4 – interface between IR camera and excitation lamp, 5 – computer.

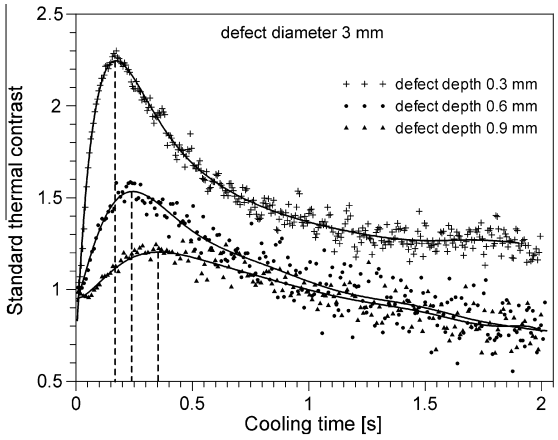

Fig. 5. Time evolution of the standard thermal contrast. Defect diameter d = 3 mm.

3.1. The method of the defect size determination

As it was mentioned, after thermal stimulation the cooling rates of the surface over the sound material and over defect are different. This difference allows detecting subsurface defects in tested material. A measure of the surface cooling rate is the time derivative of temperature. Therefore, determination of the defect size using the

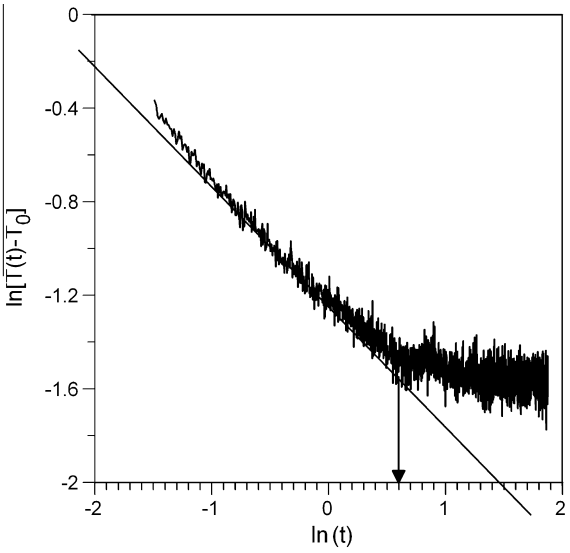

Fig. 6. Logarithmic temperature difference vs. logarithmic time evolution.

surface distribution of the time derivative of temperature instead of the surface temperature distribution is used.

To obtain such distribution for each instant of cooling process, the mathematical form of the temperature vs. cooling time for each pixel is needed. This form was found from the sequence of thermal images using Automation Technology IrNDT software. Then, the surface distribution of the time derivative of the temperature as a function of the cooling time was calculated. The results of such operation for defects diameter of 5 mm located at the different depths at the time 0.3 s after thermal excitation are presented in form of a gray field in Fig. 8. The field corresponds to the levels from 0 to 255 conventional dimensionless units. Level 0 corresponds to black and the 255 to white color.

The distribution of gray degree along straight line segment (see Fig. 8) through the center of the visible trace of selected simulated defect is presented in Fig. 9. Such distribution was used to estimate the defect diameter. Taking into account the IR camera to specimen distance and lens parameters the pixels were converted into the millimeters. In order to determine the defect diameter the tangents to the both profile arms at the half of its height were drawn. The distance between intersection points of these tangents with the

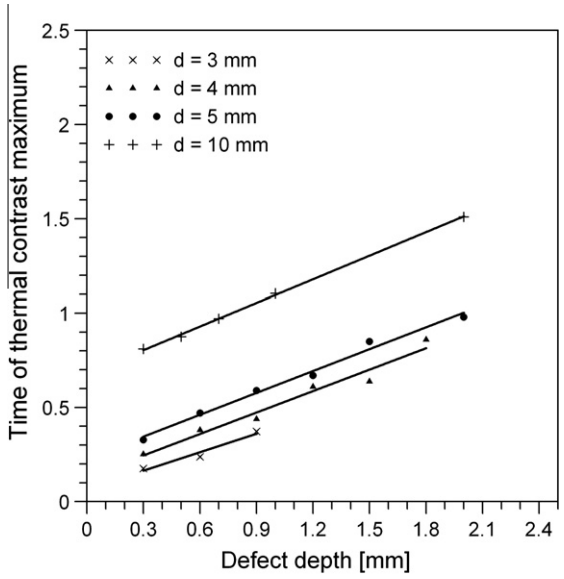

Fig. 7. Dependence of depth vs. time of thermal contrast maximum (the calibration relations).

lines related to the average values of temperature derivative over the sound material was taken as the defect diameter.

Linear profiles of the time derivative of temperature were determined for the time corresponding to thermal contrast maximum. This time is different for different sizes and depths of defects. The comparison of the reconstructed values of defect diameter with real ones is presented in Table 1. The reconstruction of the defect diameter is impossible if the increase in thermal contrast is unnoticeable.

On the basis of the reconstructed value of defect diameter, obtained calibration relations for given material and the time of thermal contrast maximum, the defect depth can be estimated. In order to verify the presented approach, the defects, in form of flat bottom holes, were made in the 5 mm thick plate of austenitic steel. The defects diameter was equal to 4 mm at the depths of: 0.3, 0.5, 0.7, 0.9, 1.2 mm. The experimental conditions were the same as that described previously in Section 2. The experiment was performed three times. The standard thermal contrast vs. cooling time relations were obtained for each defect. The example of thermal contrast vs. cooling time is presented in Fig 10. The time corresponding to thermal contrast maximum was determined for each performed experiment. Then, using calibration dependences (Fig. 7) the defects depths were assessed. The obtained results compared with real defect diameters are presented in Table 2. It is seen that presented approach gives satisfactory results.

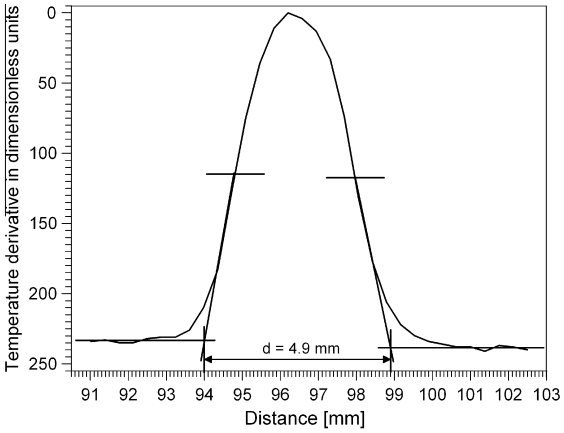

Fig. 9. Line profile of the time derivative of the temperature used for defect diameter determination.

Table 1
Comparison of reconstructed defect diameters with real ones.

Defect diameter (mm)	Reconstructed defect depth (mm)	Real defect depth (mm)
0.3	2.95	3
0.6	3.04	
0.9	2.86	
1.2	2.97	
1.5	2.70	
1.8	–	
2.0	–	
2.5	–	
0.3	4.01	4
0.6	4.00	
0.9	3.97	
1.2	3.98	
1.5	4.08	
1.8	4.16	
2.0	–	
2.5	–	
0.3	4.90	5
0.6	5.00	
0.9	5.03	
1.2	5.00	
1.5	5.00	
1.8	4.92	
2.0	–	
2.5	–	
0.3	10.01	10
0.5	9.99	
0.7	10.00	
1.0	10.01	
2.0	9.85	
3.0	10.03	
4.0	–	

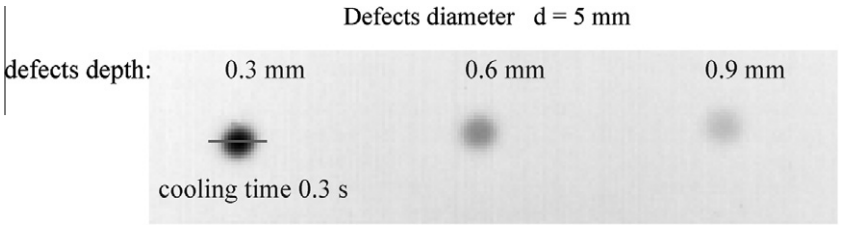

Fig. 8. Surface distribution of the time derivative of temperature. Defect diameter 5 mm, time 0.3 s.

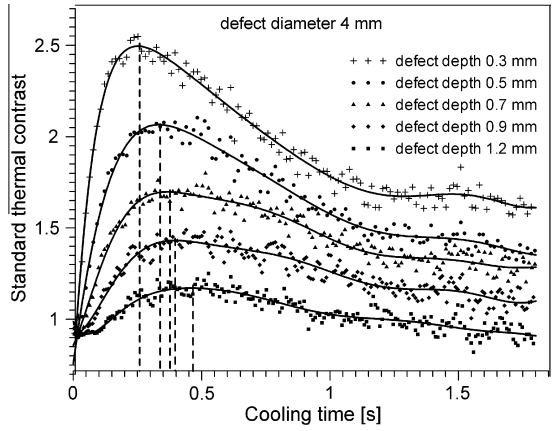

Fig. 10. Time evolution of the standard thermal contrast. Defect diameter d = 4 mm.

Table 2
Comparison of reconstructed defect depths with real ones.

Defect diameter (mm)	Reconstructed defect depth (mm)				Real defect depth (mm)
	Experiment 1	Experiment 2	Experiment 3	Experiment mean value	
4	0.30	0.28	0.32	0.30	0.30
	0.45	0.50	0.52	0.49	0.50
	0.67	0.66	0.65	0.66	0.70
	0.90	0.91	0.90	0.903	0.90
	1.20	1.19	1.20	1.196	1.20

4. Concluding remarks

It has been shown that it is possible to determine the defect size and its depth using two independent experimental methods. The methods have been used to reconstruct the size and depth of simulated defects in austenitic steel made in form of flat-bottom holes with different diameters and depths. The defect size was reconstructed from distribution of the time derivative of the surface temperature. Then, the defect depth was assessed from the dependence of the standard thermal contrast vs. cooling time. It has been shown that presented approach gives satisfactory results.

In the present work experiments were performed on the specimen of relatively high thermal diffusivity, what requires the analysis of phenomena occurring in short time intervals. Use of the proposed methods for testing of insulating materials seems to be more modest challenge. The presented experimental results may be helpful to validate numerical heat transfer model for specimen with subsurface defects. Such models allow examination of defects of different geometries without performing expensive and laborious experiments.

Acknowledgment

This work has been supported by Council of Science (Poland) under Grant No. N N501 0094 33 (2007–2010).

References

[1] H.D. Benitez, C. Ibarra-Castanedo, A.H. Bendada, X. Maldague, H. Loaiza, E. Caicedo, Definition of a new thermal contrast and pulse correction for defect quantification in pulsed thermography, Infrared Phys. Technol. 51 (2008) 160–167.
[2] M. Krishnapillai, R. Jones, I.H. Marshall, M. Bannister, N. Rajic, NDT using pulsed thermography: numerical modeling of composite subsurface defects, Compos. Struct. 75 (2006) 241–249.
[3] M. Pilla, M. Klein, X. Maldague, A. Salerno, New absolute contrast for pulsed thermography, in: D. Balageas, G. Busse, G.M. Carlomagno, S. Svaić (Eds.), Proc. 6th Int. Conf. Quant. IR Therm., Dubrovnik, Croatia, 2002, pp. 53–58.
[4] D.A. Gonzalez, C. Ibarra-Castanedo, J.M. Lopez-Higuera, X. Maldague, New algorithm based on the hough transform for the analysis of pulsed thermographic sequences, NDT E Int. 39 (2006) 617–621.
[5] S. Lungin, U. Netzelmann, An effective compression algorithm for pulsed thermography data, NDT E Int. 38 (2005) 485–490.
[6] S. Lugin, U. Netzelmann, A defect shape reconstruction algorithm for pulse thermography, NDT E Int. 40 (2007) 220–228.
[7] J.G. Sun, Analysis of pulsed thermography methods for defect depth prediction, J. Heat Transfer 128 (2006) 329–338.
[8] A.R. Hamzah, P. Delpech, M.B. Saintey, D.P. Almond, An experimental investigation of defect sizing by transient thermography, Insight 38 (1996) 167–171.
[9] X.P.V. Maldague, Theory and Practice of Infrared Technology for Nondestructive Testing, Willey-Interscience, New York, 2001, pp. 198–199.
[10] M. Suśa, Numerical modelling of pulse thermography experiments using finite elements for purposes of defect characterization, Doctor's Thesis, Quebec, Canada, 2009. pp. 82–89.
[11] M. Maj, W. Oliferuk, O. Wysocka, Relation between defect depth and standard thermal contrast on the steel surface in pulsed thermography, in. B. Więcek (Eds.), Proc. 9th Int. Conf. Quant. IR Therm., Krakow, Poland, 2008, pp. 627–631.
[12] C. Deemer, J.G. Sun, W.A. Ellington, S. Short, Front-flash thermal imaging characterization of continuous fiber ceramic composites, OSTI, ANL/ET/CP-97040 (1999) 1–7.
[13] H.X. Favro, X. Han, Y. Wang, P.K. Kou, R.L. Thomas, Pulse-echo thermal wave imaging, in: D.O. Thompson, D.E. Chimenti (Eds.), Rev. Prog. Quant. Nondestruct. Eval, Plenum Press, New York, 1995, pp. 425–430.
[14] H.S. Carslaw, J.C. Jaeger, Conduction of Heat in Solids, second ed., Oxford at the Clarenton Press, London, 1959.
[15] V.P. Vavilov, T. Ahmed, H.J. Jin, L.R. Favro, L.D. Thomas, Experimental thermal tomography of solids by using the pulse one-side heating, Sov. J. Nondestruct. Test. 12 (1990) 60–66.
[16] I. Boras, S. Svaic, A. Galovic, Mathematical model for simulation of defects under a material surface applied to thermographic measurements, in: D. Balageas, G. Busse, G.M. Carlomagno (Eds.), Proc. 4th Conf. Quant. IR Therm., Lodz, Poland, 1998, pp. 53–58.